Finite element analysis of kinematic behavior of cyclist and performance of cyclist helmet for human head injury in vehicle-to-cyclist collision

Daisuke Ito, Hidefumi Yamada, Keiji Oida and Koji Mizuno

Abstract The purpose of this study is to understand the injury mechanism of the cyclist's head and lower extremity in car-to-cyclist accidents. The kinematic behavior of the whole body and the interaction of car, cyclist and bicycle were numerically investigated using a simulation with FE models of the human, bicycle and car. In addition, protection performance of a helmet for A-pillar impact was examined with FE models of a human head, a helmet and a car. The upper body of the cyclist dropped toward the bonnet with the hip rotating on the bonnet and the upper body twisting due to the interaction between the front structure of the car and bicycle. The knee of the cyclist made contact with the bonnet leading edge and shear loading was generated resulting in ruptured knee ligaments. It was found from head impact simulations that the liner of the helmet deformed locally and bottomed out in high speed impact and as a result, high deceleration on the headform impactor was generated despite wearing the helmet. However, the helmet can prevent skull fracture and brain strain significantly. Therefore, it is concluded that there is a potential that helmets can protect the head in impacts against the A-pillar.

Keywords Cyclist and pedestrian kinematics, Cyclist impact simulations, Finite element analysis, Cyclist helmet performance

I. INTRODUCTION

In Japan, the number of cyclist fatalities and casualties in traffic accidents in 2012 were 563 (12.7% of the total traffic deaths) and 131,762 (15.9%), respectively [1]. Recently, the Japanese national police agency issued an official notice for promotion of comprehensive measures to improve the bicycle traffic control system (Japanese national police agency official notice: Act No.85 etc., 2011), and it was confirmed that, in principle, cyclists should travel not on a sidewalk but instead on a roadway. It can, therefore, be predicted that the number of car-to-cyclist collisions will likely increase in the future because of increased risk of collisions involving cyclists as well as larger numbers of cyclists due to the recent growing awareness of environmental issues.

Cyclists and pedestrians are vulnerable road users and they sustain severe injuries in motor vehicle accidents. Head, upper extremities and lower extremities are the most frequently injured body regions in cyclist accidents [2-3]. In particular, 64% of cyclist fatalities in 2009-2011 were injured in the head region [3]. Head impact can lead to serious and fatal injuries. Due to complicated kinematics of cyclists involved in collisions various patterns of head injuries are observed. For example, data on forty-nine victims involved in car-to-cyclist collisions showed that, of cyclists who sustained a single head impact, the frontal, parietal and occipital regions were injured at almost the same frequency [4]. The lower extremity also sustained various injuries. It is known that ankle and knee injuries of cyclists depend on impact direction and bumper height of cars [5]. For evaluating and improving cyclist protection, it is necessary to understand the kinematic behavior and the types of injuries to cyclists in car-to-cyclist accidents and to apply the information to develop suitable countermeasures and their test and evaluation procedures for cyclists' protection.

Many researchers have investigated cyclist kinematic behavior and injury mechanism by computer simulations. Numerical parametric studies [6-7] showed that vehicle impact velocities and impact locations are the two major factors that affect injury severity. Many research studies have shown that cyclists' kinematic behavior is comparable to that of pedestrians [8]. By contrast, Maki et al. [9] showed utilizing real-world accident investigations and multi-body simulations that in an impact with a bonnet-type vehicle, a cyclist slides over the bonnet top and this is not observed in the case of pedestrians. In the same way, Peng et al. also assessed head injury risk using reconstruction of accidents by multi-body simulation [10]. They found that

D. Ito is an assistant professor (tel: +81-52-788-6233, ito@mech.nagoya-u.ac.jp), H. Yamada and K. Oida are graduate students and K. Mizuno is a professor, all in the Department of mechanical science & engineering at Nagoya University, Japan.

cyclists suffered less severe injuries due to low head impact velocities compared to the severity of pedestrian injuries, particularly to the head and legs. The injury mechanism of the lower extremities of cyclists was investigated with finite element analysis of car-to-bicycle accidents [11]. In such cases, the bonnet leading edge hitting the upper tibia generates knee shearing and rupture of the anterior cruciate ligament (ACL).

Although crash protection performance of vehicles in pedestrian crashes is being improved by introducing regulatory or NCAP impact tests and developing new safety countermeasures, little attention has been paid to cyclist protection. For decreasing cyclist fatalities and casualties, it is desirable to understand how the differences in the whole body kinematic behavior between cyclists and pedestrians affect the injury mechanism of each human body region in car collisions to get optimum protection for both pedestrians and cyclists.

For head protection of cyclists, it is thought that helmets are effective. The effectiveness of cycle helmets was directly evaluated in various situations based on crash simulations with an adult human model wearing a helmet. It was confirmed that a helmet was effective in reducing the severity of head injuries sustained in common accidents [12]. The protection performance of a helmet has also been discussed based on cadaver tests [11] and from drop tests with the head of a crash test dummy [14]. Additionally, combination of experiment and simulation data [15], hospital patient data [16] and in-depth accident analysis [17] have all been used to study the effectiveness of helmets. These research results showed agreement on the effectiveness of cyclist helmets. In particular, Milne et al. [15] showed from FE simulations of drop tests of a helmeted human head model onto flat and kerb-block anvils that the injury risk is acceptable for most impact locations. On the other hand, there are contradictory questions of effectiveness and cost benefit of the helmet wearing requirement mandated by law [18-19].

In car crashes that involve cyclists, the head of a cyclist is able to make contact with various locations on the car. It is therefore necessary that head protection be evaluated taking into account impact conditions and locations associated with the whole body kinematic behavior in such crashes. While head injury risk in an impact against the windshield, which is relatively soft, is low, A-pillars have a high potential to cause severe head injuries as reported in a pedestrian study [20]. Therefore, protection performance of helmets on impacts against A-pillars needs to be evaluated.

The purpose of this study is to understand the injury mechanism of the cyclist's head and lower extremities in car-to-cyclist collisions. The kinematic behavior of the whole body and the interaction of a cyclist with a car and bicycle were numerically investigated using a simulation of a car-to-bicycle collision with FE models of a cyclist, a bicycle and a car. In addition, the protection performance of a helmet in a collision with the A-pillar was also examined with FE models of a human head, a helmet and a car.

II. METHODS

Car to cyclist Impact Simulation

Bicycle Model

An FE model of a bicycle was developed using reverse engineering. The dimensions of the surface of a bicycle were measured. The thickness of a bicycle frame was also measured at various locations and was reflected in the shell elements constructing the frame. A piecewise linear plasticity material model with mechanical properties of steel was applied to the frame model. Pedal and handlebar mechanisms were reproduced using kinematic joints; the handlebar is linked to the front tire and the left pedal is linked to the right pedal.

Simulation setup

The THUMS occupant FE model (ver. 3) which is 175 cm in height and weighs 77 kg was used as the cyclist. The human model was set to be in the posture with the right leg forward and the left leg backward and was placed on the bicycle model. Both left and right arms were positioned on the handlebar. The posture of the human model was changed by forced displacement applied to nodes of bones of the upper and lower extremities. In this simulation, the injury mechanism of the knee and the leg were the focus. These parts of the THUMS were validated from simulations based on shear and bending tests of the lower extremity [21].

In this study, an FE model of a passenger car (small sedan) was developed. The front structures in front of the B-pillar were modelled by using the measured dimensions of the surface of the car. In order to constrain the kinematics of the car except in a traveling direction, the nodes at the rear ends of the roof and side sills were constrained. The initial condition of simulation and comparison of position with a pedestrian are shown in Fig.

1. The cyclist with the bicycle was placed in front of the center of the car model and was facing laterally. In this simulation, the bicycle velocity was set at 0 km/h and the impact velocity of the car was set at 40 km/h.

In order to examine the loading on the lower extremity during impact, the interaction of the car, the cyclist and the bicycle were investigated by using contact forces.

The car model was validated based on pedestrian protection tests: adult and child headform tests and legform impact tests. The velocity of the headform impact test on the bonnet was 35 km/h and the impact angle was 65 degrees. The FE model of the TRL legform impactor was impacted on the front structure of the car at 40 km/h. The accelerations of the center of gravity of the headform and the tibia of the legform in simulations were compared with those in experiments. Validation results of simulation for headform and legform impact tests are shown in Fig.2. These results indicate that the responses of the car model were similar to those of a real car and the model can be used for the pedestrian impact tests.

In order to compare the kinematic behavior of pedestrians, simulation of a car-to-pedestrian collision at an impact speed of 40 km/h was also performed with the same car model (Fig.1). In these simulations, the heights of the pelvis were at the same level and only the postures of the lower extremities were different.

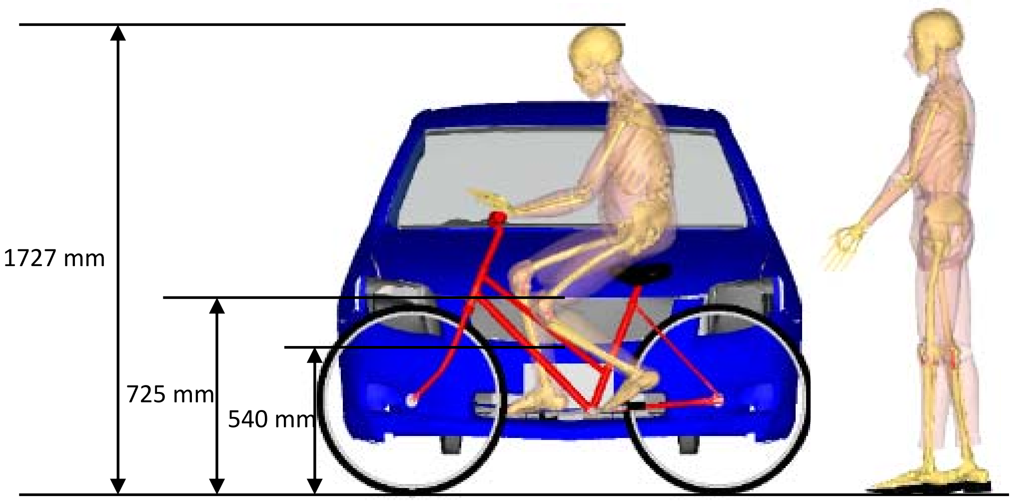

Fig. 1. Initial condition of simulation of car-to-cyclist impact and comparison of position with pedestrian.

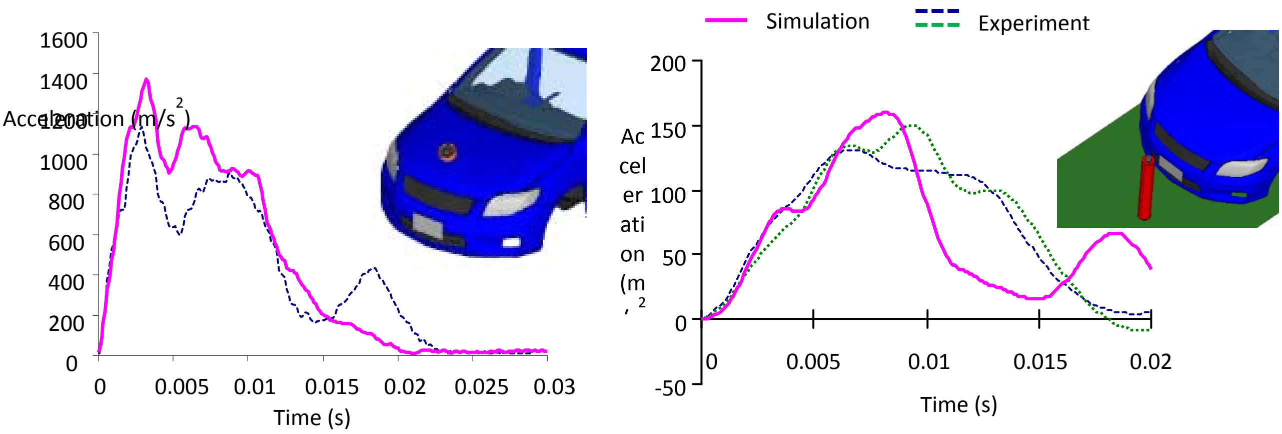

Fig. 2. Comparisons of acceleration of headform and legform impactors between experiments and simulations.

Car to head with helmet Impact Simulation

Helmet Model

An FE model of a junior cyclist helmet was developed from reverse engineering. The dimensions of the surface of the helmet were measured. The helmet consists of two parts: outer shell made of plastic material and inner liner for energy absorption. As shown in Fig. 3, the outer shell and the inner liner were modelled by shell elements and solid elements, respectively. The material properties of the inner liner were determined by drop testing of specimens extracted from the components.

In order to validate the helmet model, the simulation of drop tests onto a rigid plane was performed. The adult headform model (4.5 kg) with the helmet model was dropped from its vertex at a height of 1.5 m. The impact velocity was 5.42 m/s (19.5 km/h). A gap of 10 mm was provided between the helmet and the headform in order to reproduce the drop test situation. The acceleration of the headform in the simulation agreed with that of the experiment. From this result, it was assumed that the FE model of the helmet was validated.

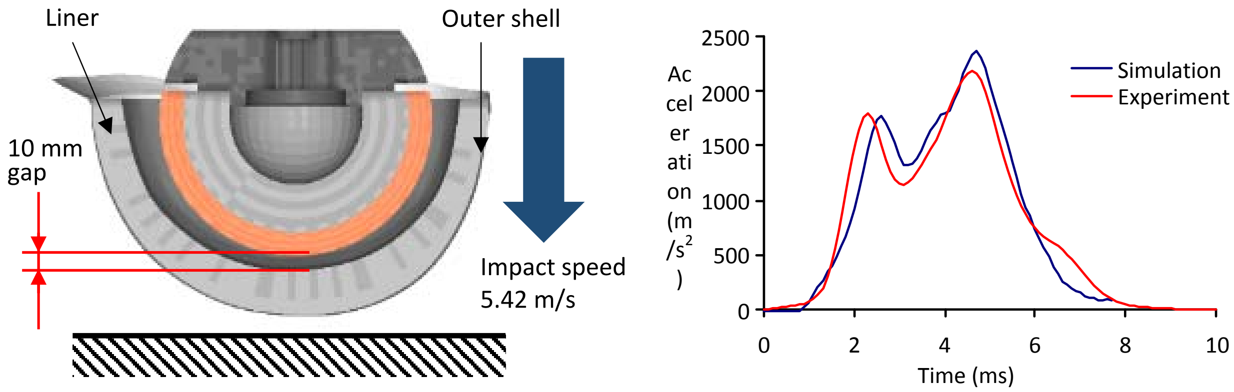

Fig. 3. Helmet model and result of validation test.

Simulation setup for car-to-head impact tests

In order to investigate the cyclist helmet performance when a cyclist's head impacts against an A-pillar which has a high potential to cause severe head injury [20] to a human head, simulations of impact tests using the head of a human FE model on an A-pillar were conducted. The head impact velocity, velocity direction and head posture were determined based on the head contact condition in the cyclist whole body kinematics in the car-to-cyclist impact simulation. For calculation of HIC, headform impact tests under the same impact condition were performed.

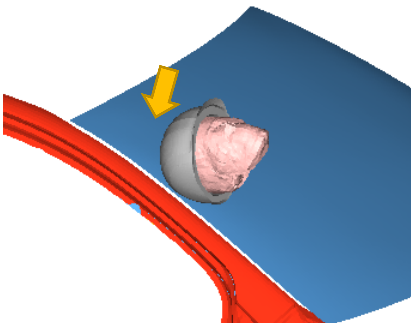

Fig. 4. Simulation setup of head impact on A-pillar.

III. RESULTS

Car to cyclist Impact Simulation

The kinematic behavior of the cyclist in an impact against the car is shown in Fig.5. Fig. 6 shows the contact force between the car, the cyclist and the bicycle in order to examine the loading on the lower extremity during impact. Cross sections were defined at intervals of 20 mm for measurement of section forces and moments. Bending moment on the right tibia is also shown in Fig. 6. The sign of the bending moment was defined to be positive when the lower extremity bent along the front shape of the car. The bending moment drawn in Fig. 6 is measured at the cross-section which is 0.27 m from the distal end of the right tibia. This cross-section at 0.27 m has the highest peak of all measured cross-sections of the right leg.

Initially, the right leg made contact with the bumper. Until 10 ms (milliseconds), the tibia was bent medially due to the contact with the bumper. Then, the right knee started to impact the bonnet leading edge. The distal site of the leg was caught between the bumper and the frame of the bicycle. The bicycle pushed the leg backward of the car model. At the same time with the contact between the leg and the bicycle, the upper body rotated around the vertical axis with the right knee as pivot. As a result, the upper body, pelvis and right thigh started to rotate around the right knee and the cyclist begins to sit upon the bonnet (15 ms). At this time, the right leg started to bend laterally as shown in Fig. 6 (positive bending moment). In this phase, the proximal site of the right leg was stopped first due to the shape of the bonnet leading edge, whereas the distal site of the femur moved in a rearward direction of the car model. As a result, shear loading was generated in the right knee, and the anterior cruciate (ACL) and the medial collateral ligaments (MCL) were ruptured at 15 and 25 ms, respectively (Fig. 7). After 50 ms, the right leg rebounded from the bumper. The upper body dropped toward the bonnet with the hip rotating around the vertical axis on the bonnet and the upper-body twisting. The occipital region of the head then impacted on the windshield after contact between the elbow and the windshield (130 ms). The windshield was

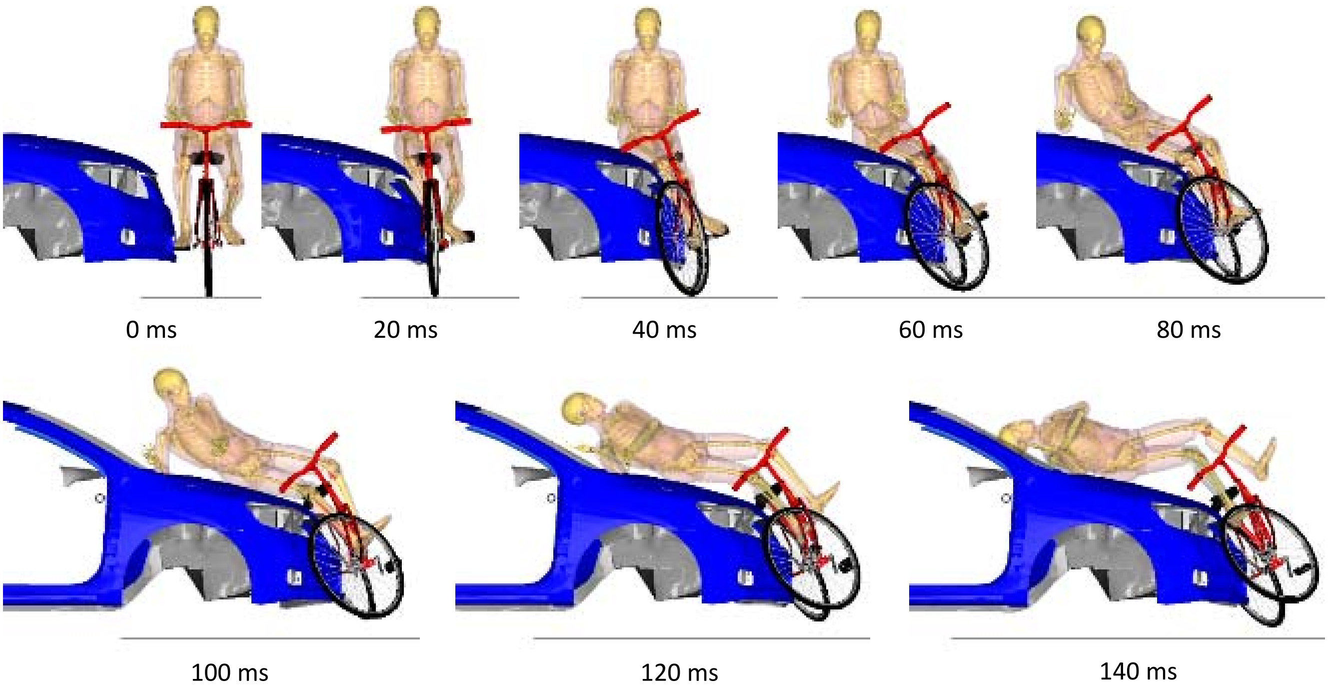

Fig. 5. Cyclist Kinematic behavior in a collision of the car model (40 km/h).

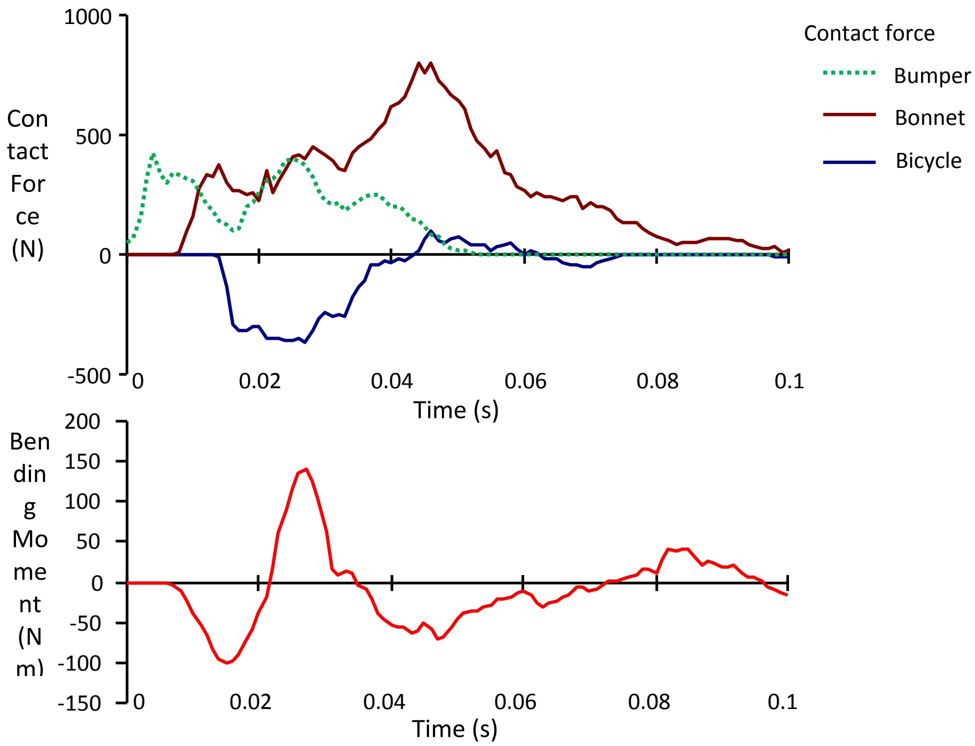

Fig. 6. Contact forces and bending moment on the right leg.

soft and it deformed thus preventing a likely skull fracture.

The kinematic behavior of the cyclist was examined and compared to that of the pedestrian. Fig. 8 shows the kinematic behavior of the pedestrian. First, the right leg made contact with the bumper of the car. Similar behavior to that observed in the case of the cyclist was seen until the hip of the pedestrian was struck by the bonnet leading edge. Then, the upper body wrapped and rotated laterally along the contour of the front of the car, and the thorax and the head made contact with the bonnet top at 104 ms and with the windshield at 120 ms, respectively.

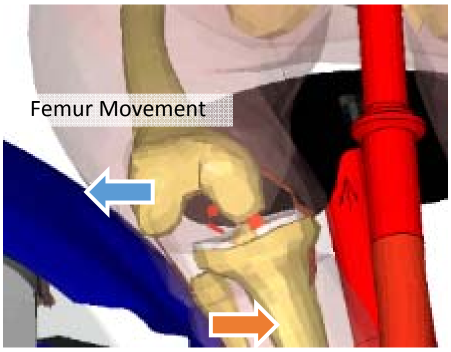

Fig. 7. Shear deformation in the right knee (20 ms).

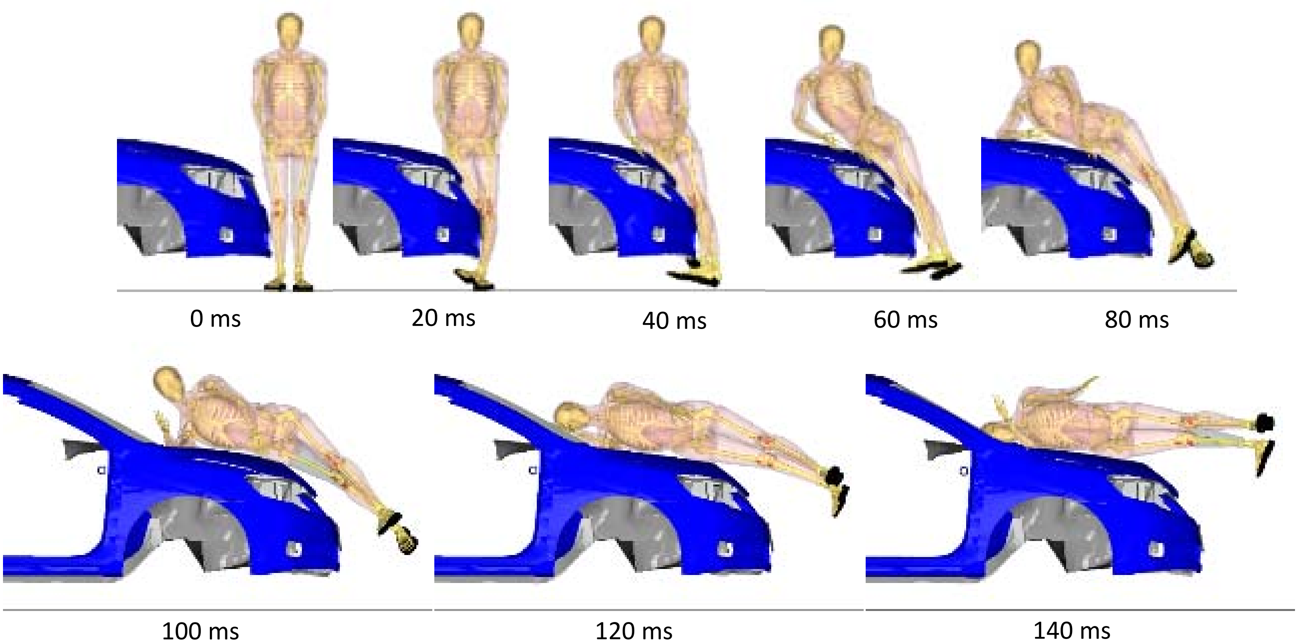

Fig. 8. Kinematic behavior of pedestrian in a collision of the car model (40 km/h).

A significant difference in the kinematic behavior between the cyclist and the pedestrian was observed in the motion of the upper body. The upper body of the cyclist moved towards the bonnet with the pelvis rotating on the bonnet and thus twisting the upper body. On the other hand, the upper body of the pedestrian bent laterally without the rotating motion of the body around the vertical axis. In these two simulations, the heights of the pelvis were at the same level and only the postures of the lower extremities were different. It is indicated that the flexion angle of the hip joint resulted in interaction between the bonnet leading edge and posterior side of the right thigh of the cyclist. In addition, the leg was caught between the front of the car and the frame of the bicycle and worked as a pivot, resulting in the twisting motion of the upper body (Fig. 9).

The effects of the lower extremity position and the contact force from the bicycle on the tibia were examined by using the bending moment diagram of the right tibia (Fig. 10). In the cyclist leg, the bending moment due to contact with the bumper was positive and that on the rest of the leg was negative at 10 ms. After that, the cyclist's leg bent laterally (positive bending side). The pedestrian leg substantially bent laterally (positive side). The maximum bending moment was 354 Nm which exceeded the injury threshold (human tibia bending moment at 50% probability of fracture is estimated as 312 Nm [22]). The moment near the proximal end of the leg of the pedestrian was high, which indicated loading due to bending was applied to the knee of the pedestrian.

The maximum and minimum bending moments of the cyclist were smaller than those of the pedestrian. One difference is that the leg of the cyclist bent medially due to the impact with the bumper while the leg of the pedestrian bent laterally from impact timing. In the maximum bending phase, the bending moment of the cyclist at the proximal end was smaller than that of the pedestrian. It is reasonable to assume that the knee of the cyclist was mainly subjected to shear loading, and the bending moment generated by the thigh and the upper body was not transmitted to the leg through the knee.

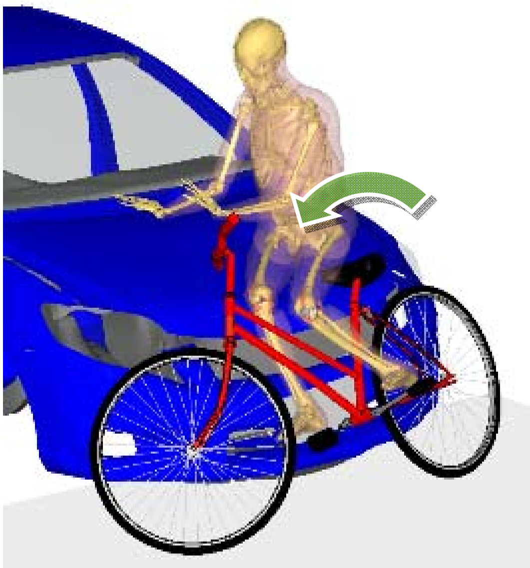

Fig. 9. Rotating motion of the thigh and pelvis on the bonnet top.

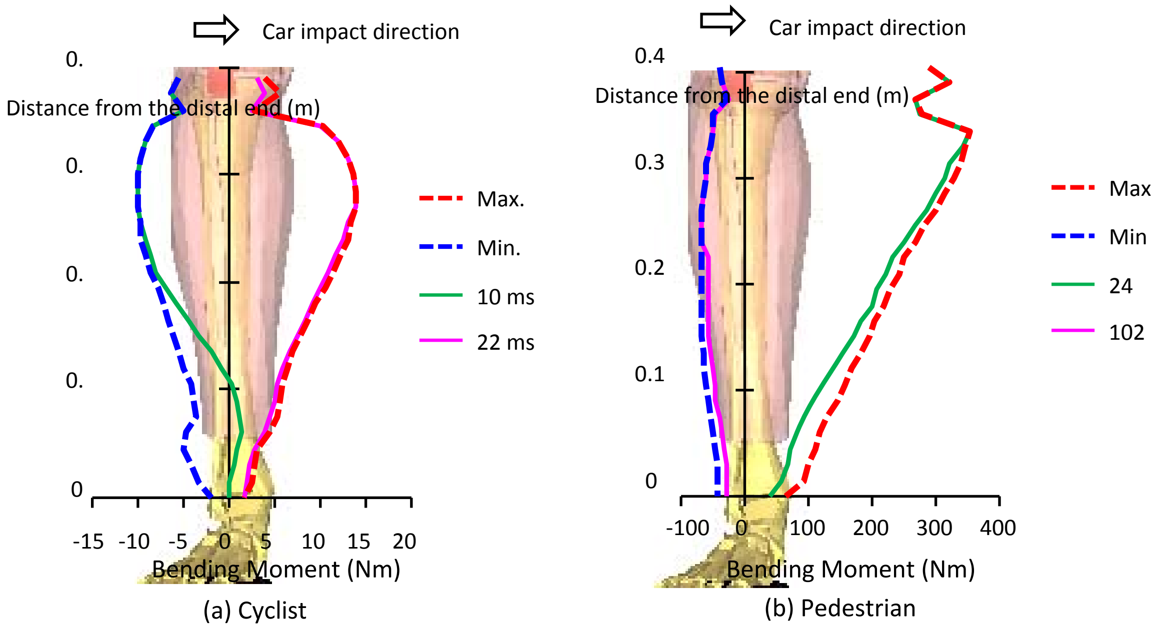

Fig. 10. Bending moment diagrams of cyclist and pedestrian tibia in a collision with the car model (40 km/h). In these figures, the sign of the bending moment was defined to be positive when the leg bent along front shape of car.

In order to examine the bending motion of the right leg of the cyclist, schematic diagrams are shown in Fig. 11. At 10 ms, the right leg bent medially except at the contact area with the bumper as shown in Fig. 10. The leg had made contact with the bumper and started to make contact with the bonnet leading edge. It is reasonable to assume that this bending occurred due to the inertial force. At 20 ms, the leg tended to bend along the contour of the car front shape. The frame of the bicycle hit on the distal side of the leg and the contact force was generated in the opposite direction against the contact forces from the bumper and the bonnet leading edge. The force may act as a cancelling force for positive bending moment on the right leg of the cyclist.

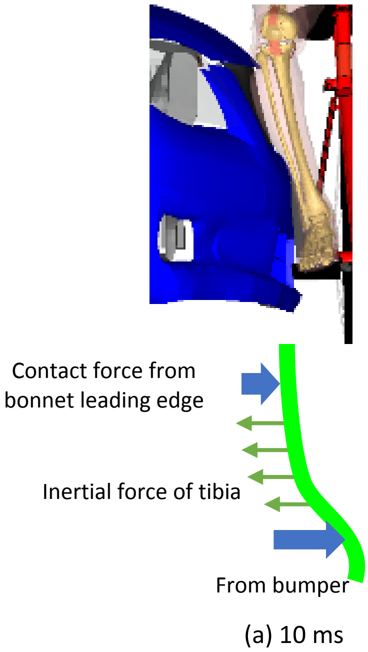

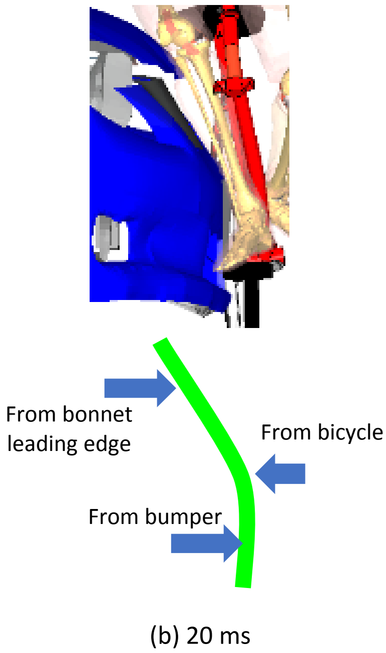

Fig. 11. Schematic diagram of loading condition of the right leg of the cyclist at 10 ms and 20 ms.

Trajectories of the head, thorax, pelvis and right knee of the cyclist and the pedestrian at an interval of 20 ms are shown in Fig.12.The hip and thigh of the cyclist travelled onto the bonnet and the upper body kept its initial posture substantially until 50 ms. At this time, slight lateral rotation around the hip was observed. After that, the hip and thigh slid over the bonnet top and the thorax and the pelvis moved rearward of the car while the height of these body regions remained nearly at their initial height. The travel direction of the head of the cyclist changed in vertical direction gradually after 60 ms.

In the pedestrian collision, the upper body wrapped and rotated laterally along the contour of the front of the car as shown earlier in Fig. 8. The head trajectory was different between the cyclist and the pedestrian in the coronal plane. The head of the cyclist moved horizontally until 40 ms while that of the pedestrian moved vertically after 20 ms. As a result, the head impact location was closer to the cowl in the pedestrian collision than in the cyclist collision. The moving distance towards the rear of the car of the pelvis of the cyclist was larger than that of the pedestrian. This is because the pelvis moved horizontally due to the rotating motion of the pelvis on the bonnet top. This result indicates that the difference in the motion of the pelvis on the bonnet top results in the trajectories shown. The distances that the cyclist's head and thorax moved were larger than those of the pedestrian.

The time histories of head resultant velocity relative to the car are shown in Fig. 13. Until 50 ms, the head velocity was constant. After that, the velocity increased until about 110 ms and then started to decrease. The time history of the cyclist's head velocity was similar to that of the pedestrian. The occipital region of the head made contact with the windshield at 135 ms. The head velocity was 11.6 m/s (41.8 km/h) when the head made contact with the windshield and the impact angle was 55 degrees.

Car to head with helmet Impact Simulation

In this simulation, the data from the headform impact test were used to calculate the HIC. Fig. 14 shows the accelerations of the headform with and without the helmet in impact against the A-pillar. In the headform test without the helmet, the acceleration reached its peak at 3 ms after contact. In contrast, the headform with the helmet had two peaks. The first peak seen in Fig. 14 was due to the contact with the rebounded helmet and the second peak was due to the bottoming out of the liner. The A-pillar was so stiff that the liner deformed locally

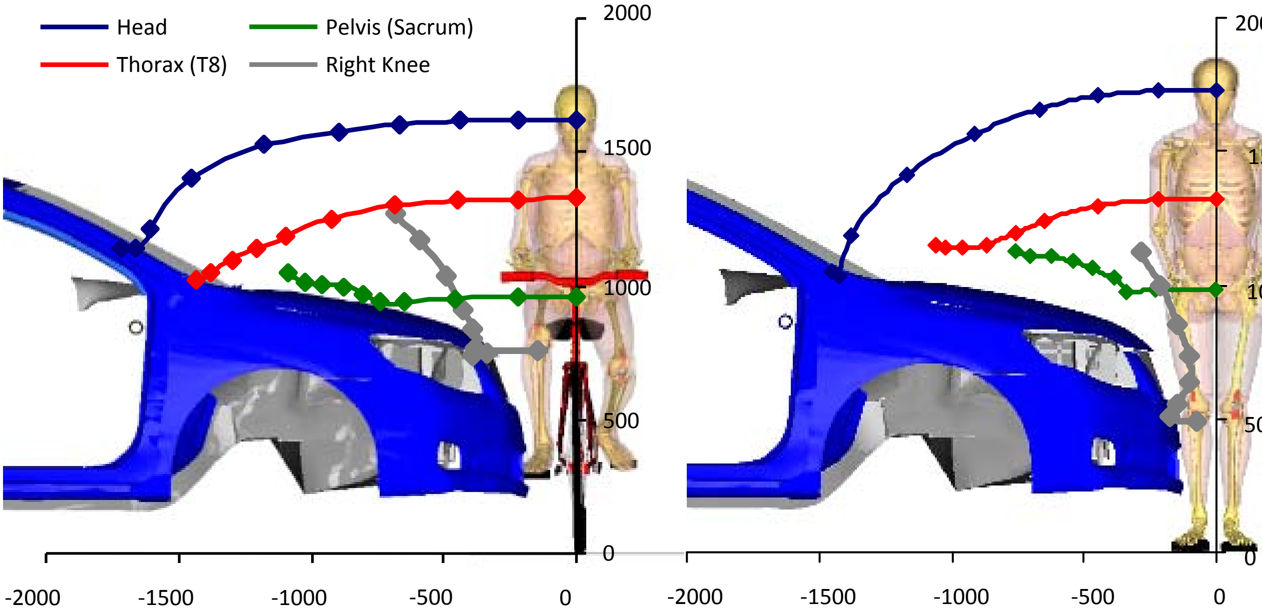

Fig. 12. Trajectories of head, thorax, pelvis and knee.

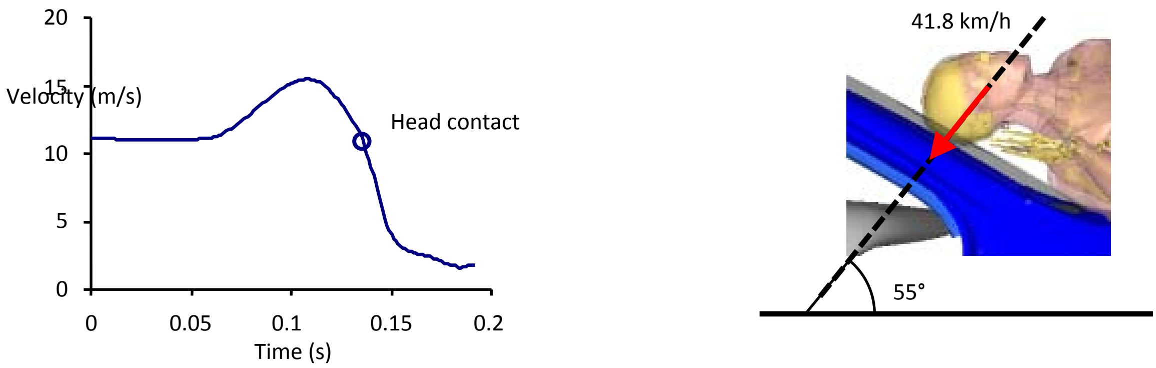

(a) Head relative speed to the car (b) Head impact angle

Fig. 13. Head relative speed to the car and impact angle.

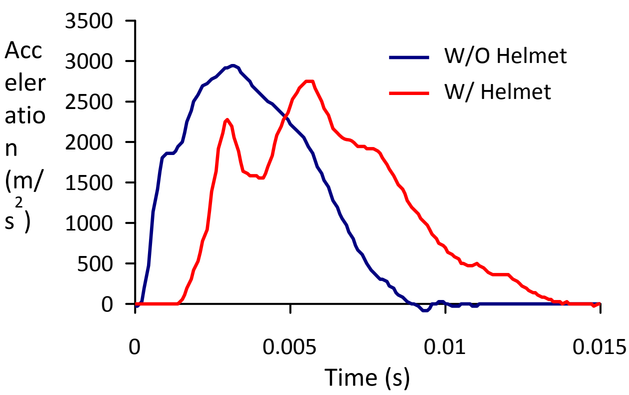

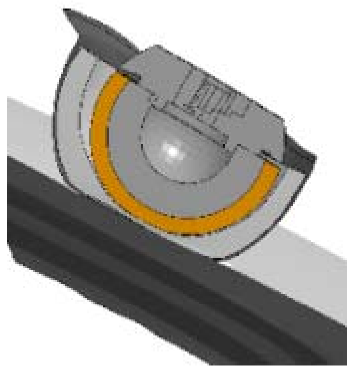

Helmet deformation at 7 ms

Fig. 14. Head accelerations of headform impactor in a collision against A-pillar.

and substantial bottoming out occurred. As a result, the high acceleration was generated in spite of wearing a helmet. The HIC values and maximum acceleration in impact on the A-pillar with and without the helmet (Table 1) were compared.

The HIC values with and without the helmet were 3881 and 4923, respectively. The helmet could thus reduce the head acceleration by 6% and the HIC by 21%. However, even with the helmet, the acceleration and the HIC values were still very high and exceeded the HIC injury threshold (1000).

TABLE I
THE HIC VALUES IN IMPACT ON A-PILLAR

	HIC	Max. Acceleration (m/s^2)
With Helmet	3881	2751
Without Helmet	4923	2937

The head of the human FE model was also impacted against the A-pillar in order to examine the head injury potential for skull fracture and brain damage. The distributions of maximum shear strain in the horizontal plane of the head are shown in Fig. 15. In the head without the helmet, skull fractures occurred at 2 ms after contact and spread over a wide area of the skull. After that, the brain was deformed substantially along the shape of the A-pillar. On the other hand, the helmet prevented local deformation of the skull and the brain in the area of contact. Small strain was measured in the skull and the skull fracture did not occur in the impact when the helmet was worn. Although the strain in the vicinity of longitudinal fissure of the cerebrum remained more than 10% which is a threshold of moderate diffuse axonal injury [23], these results from the headform and the human head impact tests show that the helmet could reduce not only skull deformation against impact loads but also brain strain although the head acceleration of the headform remained high.

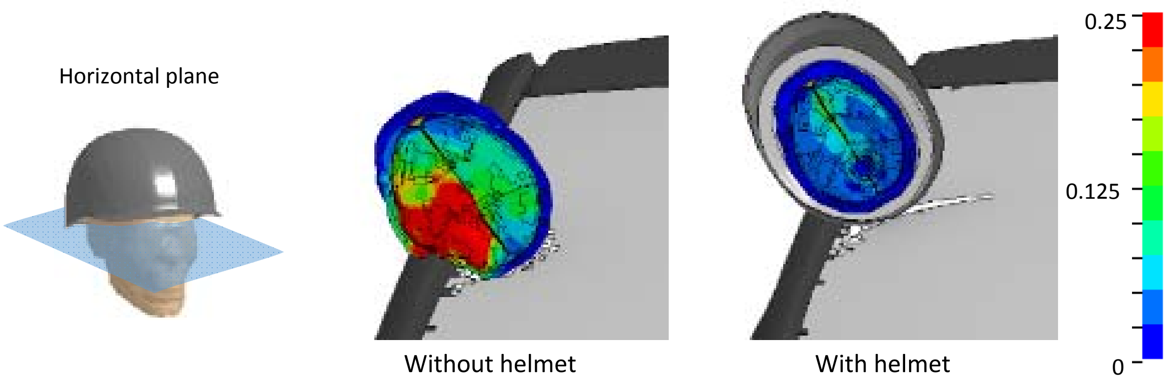

Fig. 15. Maximum shear strain in brain.

IV. DISCUSSION

In this study, simulations of a car-to-bicycle collision and a car-to-head collision with FE models of human, bicycle, car and cycle helmet were conducted. It was confirmed that the cyclist's hip rolled onto the bonnet top during impact. The kinematic behavior of the upper body and large displacement of the head are in agreement with that in the multi-body simulation study reported by Maki et al. [9] and in the FE simulation study by Cardot [11]. Such rolling behavior is not seen in our impact simulation with the pedestrian model and is not common in the pedestrian-to-sedan collision [9]. In this case, the pedestrian impacted laterally rotated around the pelvis, and the lateral side of the head and thorax struck the bonnet. The result indicates that the head of the cyclist travels further from the front end of the car than the pedestrian because of the sliding behavior and may be at a higher risk of impact with the cowl, the A-pillar, the windshield and a front part of the roof of the car. The results of this study indicate that flexion angle of the hip joint results in interaction between the bonnet leading edge and the posterior side of the right thigh of the cyclist. In addition, in our simulation, the upper body of the cyclist twisted and moved towards the bonnet. As a result, the occipital region of the head impacted the windshield. It can be assumed that the whole body kinematics strongly depends on the front shape of a car, posture and body size of the cyclist, impact location and direction of travel of the bicycle. Further research will be needed in order to investigate the effects of these factors on the kinematic behavior and injury outcomes.

It was found that the legs of cyclists are at high injury risk, especially the knee joints. Accident analysis in Germany showed that the risk of knee injury was higher for cyclists than for pedestrian [24] and about 60% of cyclists struck by the front of a car suffered bone and/or ligament injuries to the knee [25]. The knee of the cyclist in this study was subject to shear loading caused by the impact against the proximal end of the leg. As a result, ACL and MCL were ruptured. The present results are consistent with previous results that contact of the bonnet leading edge with the upper tibia of a cyclist causes lateral dislocation between the tibia and the femur [11]. We considered that the shear displacement of the knee is one possible cause of the knee injuries of the cyclist.

This injury mechanism of the knee of the cyclist is different from that of the pedestrian. In general, it is thought that pedestrian leg injury results from a bending load acting on the lower extremity. By contrast, a smaller bending moment was applied to the leg of the cyclist at an impact speed of 40 km/h in this study. Although vehicles are equipped with lower energy-absorbing structures for prevention of excessive bending of the legs of pedestrians, the lower energy absorber may not be sufficient to prevent injuries in car-to-cyclist collisions. Therefore, in addition to the front shape of a car, posture and body size of the cyclist, impact location and direction of travel of the bicycle, interaction between leg, car and bicycle also have to be considered to prevent injuries to cyclists.

In this study, simulations of a car-to-head collision at 41.8 km/h against the A-pillar with FE models of a headform impactor and a human head with a helmet were also performed. It was found that the liner of the helmet deformed locally and bottomed out and, as a result, high deceleration was generated despite wearing the helmet. In a helmet performance requirements standard [26-27], drop tests of a rigid headform with helmet are prescribed at a height of 1.5 m (equivalent velocity of 19.5 km/h). This velocity is lower than the cyclist head impact velocity (41.8 km/h) in car collisions at 40 km/h in this study. The headform impact simulation result against the A-pillar suggests that the helmet designed for the drop test does not always reduce the injury measures to less than the threshold in a cyclist head impact against a vehicle.

The simulation with a FE model of a human head showed that the helmet reduced the loading on the head effectively to prevent skull fracture but produced slightly large strain in the brain. The helmet effectiveness found in this study is in good agreement with that from a previous study [15]. In the headform test, even though the impact force from the A-pillar was distributed by the helmet liner, the force transmitted due to bottoming out of the liner resulted in high acceleration. On the other hand, distribution of the impact force led to low level stress of the skull and skull fracture did not occur. In conclusion, it is considered that a helmet is effective for A-pillar impact of the human head. Further research will be needed to understand the protection mechanism of helmets and to derive the design principles for helmets for reducing head injury.

One limitation of our research was the model validation for the car model. Although the headform accelerations from simulations were in very good agreement with those from experiments, the peak legform acceleration from simulation was higher than that from experiment. The lack of validation may slightly change the kinematic behavior and injury occurrence of cyclists. Nevertheless, our study shows that it is possible to analyze the kinematic behavior and injury mechanism by using FE simulation in detail. This can be used to improve the protection of the leg and other body parts.

V. CONCLUSIONS

In this study, car-to-cyclist impact and car-to-head impact simulations were performed by using FE models of a human, a bicycle, a helmet and a car. Significant differences in the kinematic behavior between the cyclist and the pedestrian were present in the motion of the upper body. The upper body of the cyclist moved toward the bonnet with the hip rotating on the bonnet top and the upper body twisting. As a result, the occipital region of the head made contact with the windshield. The knee of the cyclist made contact with the bonnet leading edge and shear deformation was generated in the right knee, the ACL and the MCL. These kinematic behaviors, head impact condition and knee injury mechanism of the cyclist are different from those of pedestrians. The bending moment on the right tibia of the cyclist affected the interaction between the leg and the bicycle and was smaller than that of the pedestrian. It was found from head impact simulations that the liner of the helmet deformed locally and bottomed out and, as a result, high deceleration of the headform was generated despite wearing the helmet. However, helmets can prevent skull fracture and brain strain significantly. Therefore, it is concluded that there is potential for helmets to protect the head in an impact against the A-pillar.

VI. REFERENCES

[1] The Japanese National Police Agency. Occurrence situations of the traffic accident in 2012 (in Japanese).

[2] Otte D, Jänsch M, Haasper C. Injury protection and accident causation parameters for vulnerable road users based on German In-Depth Accident Study GIDAS. *Accident Analysis and Prevention,* 2012, 44(1):149-153.

[3] Institute for Traffic Accident Research and Data Analysis (ITARDA). Wear a helmet to reduce injuries from cycling accidents. *ITARDA Information*, No. 97, 2012 http://www.itarda.or.jp/itardainfomation/english/info97_e.pdf [Access on 2014/03/14].

[4] Depreitere B, Van Lierde C, et al. Bicycle-related head injury: a study of 86 cases. *Accident Analysis and Prevention,* 2004, 36(4):561-567.

[5] Rich J, Dean DE, Powers RH (Eds.). Forensic Medicine of the Lower Extremity, pages 311-342, *Humana Press Inc.*, New Jersey, USA, 2005.

[6] Van Schijndel M, de Hair S, Rodarius C, Fredriksson R. Cyclist kinematics in car impacts reconstructed in simulations and full scale testing with Polar dummy. *Proceedings of IRCOBI Conference*, 2012, paper no. IRC-12-85, Dublin, Ireland.

[7] Fanta O, Bouček J, Hadraba D, Jelen K. Influence of the front part of the vehicle and cyclist's sitting position on the severity of head injury in side collision. *Acta of Bioengineering and Biomechanics*, 2013, 15(1): 105-112.

[8] Janssen EG, Wismans JSHM. Experimental and mathematical simulation of pedestrian-vehicle and cyclist-vehicle accidents. *SAE* paper no. 856113, 1985.

[9] Maki T, Kajzer J, Mizuno K, Sekine Y. Comparative analysis of vehicle-bicyclist and vehicle-pedestrian accidents in Japan. *Accident Analysis and Prevention*, 2003, 35(6):927-940.

[10] Peng Y, Chen Y, Yang J, Otte D, Willinger R. A study of pedestrian and bicyclist exposure to head injury in passenger car collisions based on accident data and simulations. *Safety Science*, 2012, 50(9):1749-1759.

[11] Cardot J, Masson C, Arnoux PJ, Brunet C. Finite element analysis of cyclist lower limb response in car – bicycle accident. *International Journal of Crashworthiness*, 2006, 11(2):115-129.

[12] McNally DS, Whitehead S. A computational simulation study of the influence of helmet wearing on head injury risk in adult cyclists. *Accident Analysis and Prevention*, 2013, 60:15-23.

[13] Depreitere B, Van Lierde C, et al. Lateral head impacts and protection of the temporal area by bicycle safety helmets. *The Journal of Trauma Injury, Infection, and Critical Care*, 2007, 62(6):1440-1445.

[14] McIntosh AS, Lai A, Schilter E. Bicycle helmets: head impact dynamics in helmeted and unhelmeted oblique impact tests. *Traffic Injury Prevention*, 2013, 14(5):501-508.

[15] Milne G, Deck C, Bourdet N, Carreira RP, Allinne Q, Willinger R. Development and validation of a bicycle helmet: Assessment of head injury risk under standard impact conditions. *Proceedings of IRCOBI Conference,* 2012, paper no. IRC-12-86, Dublin, Ireland.

[16] Maimaris C, Summers CL, Browning C, Palmer CR. Injury patterns in cyclists attending an accident and emergency department; a comparison of helmet wearers and non-wearers. *British Medical Journal*, 1994, 308(6943):1537-1540.

[17] Otte D, Haasper C. Effectiveness of the helmet for bicyclists on injury reduction in German road accident situations – state of affairs on GIDAS. *International Journal of Crashworthiness*, 2010, 15(2):211-221.

[18] Curnow WJ. The Cochrane Collaboration and bicycle helmets. *Accident Analysis and Prevention*, 2005, 37(3):566-573.

[19] Robinson DL. Bicycle helmet legislation: Can we reach a consensus? *Accident Analysis and Prevention,* 2007, 39(1):86-93.

[20] Mizuno K, Kajzer J. Head Injuries in Vehicle-Pedestrian Impact. *SAE World Congress,* 2000, paper no. 2000-01-0157

[21] Maeno T and Hasegawa J. Development of a finite element model of the total human model for safety (THUMS) and application to car-pedestrian impacts, *17th International Technical Conference on the Enhanced Safety of Vehicles (ESV)*, 2001, Amsterdam, Paper no 494.

[22] Kerrigan JR, Drinkwater DC, et al. Tolerance of the human leg and thigh in dynamic latero-medial bending, *International Journal of Crashworthiness*, 2004, 9 (6):607-623.

[23] Margulies SS, Thibault LE. A proposed tolerance criterion for diffuse axonal injury in man. *Journal of Biomechanics,* 1992, 25(8):917-923.

[24] Haasper C, Otte D, Knobloch K, Zeichen J, Krettek C, Richter M. Kniegelenkverletzungen des ungeschützten verkehrsteilnehmers im straßenverkehr, Der Unfallchirurg, 2006, 109 (12):1025-103.
[25] Otte D, Haasper, C. Technical parameters and mechanisms for the injury risk of the knee joint of vulnerable road users impacted by cars in road traffic accidents, *Proceedings of IRCOBI Conference*, 2005, Prague, Czech Republic.
[26] European Committee for Standardization, 1997. Helmet for pedal cyclists and for users of skateboards and roller skates. EN1078.
[27] Japanese Standards Association, 2007. JIS T8134: Protective helmets for bicycle users.